UCRL- 91693
PREPRINT
CONF-850310-- 114

A HIGH EFFICIENCY I.C.F. DRIVER EMPLOYING MAGNETICALLY CONFINED PLASMA RINGS

D. J. Meeker
J. H. Hammer
C. W. Hartman

UCRL--91693

DE85 012939

This paper was prepared for presentation at
Sixth Topical Meeting on the Technology of
Fusion Energy, San Francisco, California
March 3-7, 1985

March 4, 1985

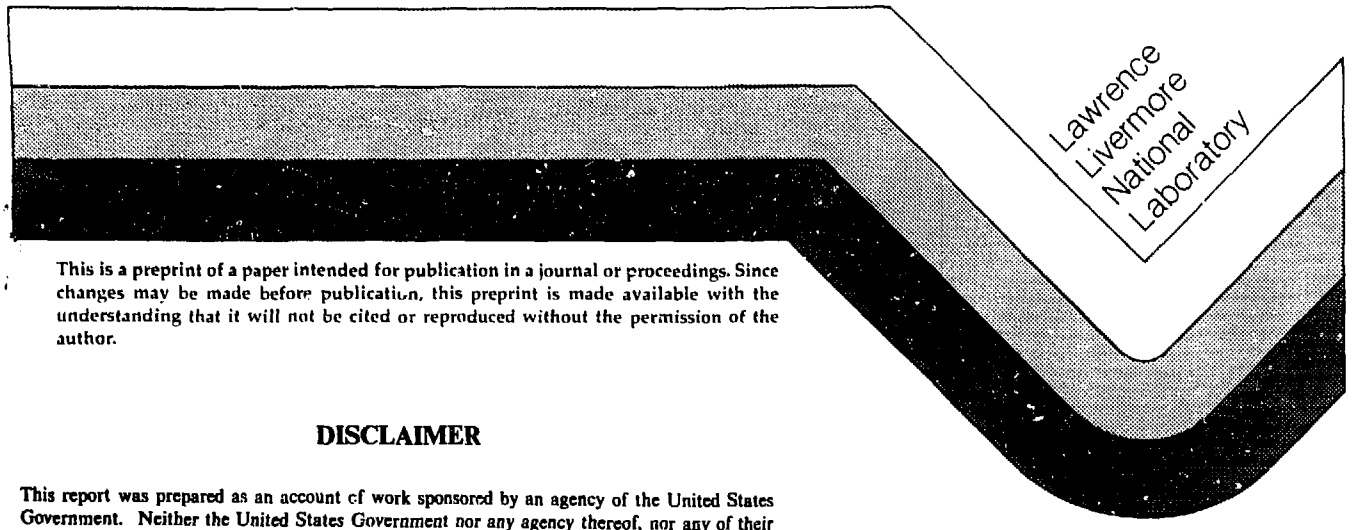

DISCLAIMER

A HIGH EFFICIENCY I.C.F. DRIVER EMPLOYING MAGNETICALLY CONFINED PLASMA RINGS

D. J. MEEKER, J. H. HAMMER, and C. W. HARTMAN, Lawrence Livermore National Laboratory
P. O. Box 808
Livermore, California 94550
(415) 422-5434

ABSTRACT

We discuss the possibility of achieving energy, power and power density necessary for ICF by magnetically accelerating plasma confined by a compact torus (CT) field configuration. The CT, which consists of a dipole (poloidal) field and imbedded toroidal field formed by force-free, plasma current, is compressed and accelerated between coaxial electrodes by B_θ fields as in a coaxial railgun. Compression and acceleration over several meters by a 9.4 MJ capacitor bank is predicted to give a 5.7 cm radius, 0.001 gm CT 5 MJ kinetic energy (10^7 m/sec). Transport and focussing several meters by a disposable lithium pipe across the containment vessel is predicted to bring 4.8 MJ into the pellet region in 0.5 cm^2 area in 0.3 ns. The high efficiency (~ 50%) and high energy delivery of the CT accelerator could lead to low cost, few hundred MW power plants that are economically viable.

INTRODUCTION

Inertial Confinement Fusion (ICF) targets that produce moderate to high fusion gains now appear to require input energies of 1-10 MJs. With present estimated costs and efficiencies of laser and charged particle drivers, one is forced into configurations of very large power plants (> 1 GW) and/or multiple reactor chambers driven by a single source to be economically viable. Unfortunately, this is counter to the present philosophy of the utility companies, who now encourage construction of smaller, less capital intensive plants to increase generating capacity. A solution to this problem is a highly efficient, inexpensive driver that can deliver MJ's of energy in the high power density form required by ICF targets. Compact toroids that are accelerated by existing capacitor banks or Marx stages appear to meet this need.

General Description of the Approach

The compact toroid accelerator is based on the magnetic plasma confinement configuration, the compact torus (CT), sketched in Fig. 1. A CT consists of a toroidal magnetic structure containing both toroidal (azimuthal) and poloidal (perpendicular to the azimuthal direction) magnetic fields. The field lines map out closed surfaces so that particles and energy are well confined. CT's produced by a magnetic plasma gun are typically low pressure ($\beta = 8\pi P/B^2 >> 1$) and hence nearly force free ($\nabla \times \underline{B} = k\underline{B}$). The formation of a compact toroid by a magnetized plasma gun is shown schematically in Fig. 2. The large force-free currents in the compact toroid are primarily responsible for the ring magnetic fields making the ring self-contained, as opposed to other devices such as the tokamak, which have an applied toroidal field with external currents linking the torus. All magnetically confined plasmas require some external force to prevent a radial expansion. For the compact toroid this is usually supplied either by an applied axial magnetic field or simply by image currents in conducting surfaces.

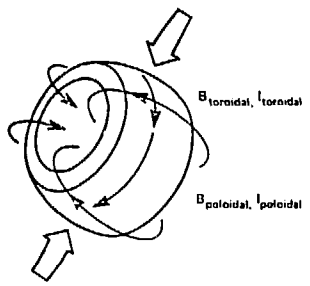

Figure 1

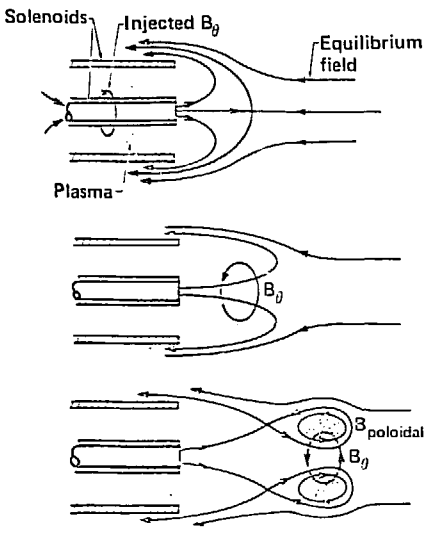

Figure 2

CT's have been produced in several ways,[1,2,3] we concentrate here on results obtained using the magnetized plasma gun. Recent experiments[4,5] have used 100 kJ energy plasma guns to produce CT's having magnetic energies of 1-10 kJ. The CT's have typical dimensions R = 40 cm, a = 20 cm (R/a = major/minor radius) defined by the pill-box flux conserver into which they are injected. Depending on the plasma density, the total mass of the CT ranges from about 5×10^{-6} to 5×10^{-4} gm. Without special impurity control, roughly one half the CT mass is composed of oxygen and carbon impurity ions. Impurity control can nearly eliminate carbon and reduce the oxygen ion concentrations to several percent.

Stable decay is obtained for appropriately shaped flux conservers and compact toroid lifetimes are limited by ohmic decay of the magnetic field, scaling approximately as the classical lifetime, $\tau_{decay} \propto R^2 T_e^{3/2}/Z_{eff}$, where T_e is the electron temperature, and Z_{eff} is the average charge state. The observed particle-confinement times are similar to the magnetic decay time. Without impurity control, the electron temperature remains clamped at about 10 eV by low-Z impurity radiation, resulting in τ_{decay} values of about 100 μs for a typical compact toroid. In recent experiments at LANL,[6] researchers succeeded in controlling impurity concentrations, the result being that the peak T_e exceeds 150 eV and τ_{decay} is about 1 ms. For purposes of acceleration, 10 eV rings are usually sufficiently long lived because $\tau_{acceleration} < 10$ μs. Generally, under conditions for which CT's have been formed, ohmic heating is sufficient to maintain $T_e > 10$ eV for any ion species with Z_{eff} being of the order $Z_{eff} \simeq 3$. Consequently, a decay rate similar to that obtained without impurity control would be expected, allowing acceleration of any species ion.

There are many ways to magnetically accelerate a CT. In this paper we use the coaxial railgun configuration where the ring acts as a sliding short and the magnetic pressure behind the ring provides the accelerating force. The coaxial railgun offers the virtue of simplicity and the possibility of inductive magnetic energy storage when compact toroid acceleration is preceded by a compression phase. The coaxial mode is also a natural extension of the formation technique using a magnetized coaxial plasma gun to create the compact toroid. A coaxial railgun accelerator and compression section is sketched in Fig. 3.

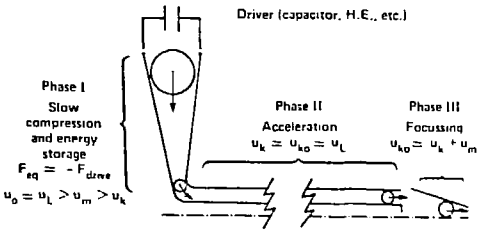

Figure 3

The sequence of events in the acceleration process is as follows:

1) Gas is puffed into the gun, and the gun bank is fired, ionizing the gas and forcing plasma and toroidal magnetic flux through the pre-established poloidal field of the gun. This is the well established plasma-gun formation technique for a compact toroid, as depicted in Fig. 2 and the result is a compact toroid at the beginning of the acceleration/compression section. Ring mass is controlled by varying the amount of gas initially injected.

2) The acceleration bank is fired through a second coaxial feed, introducing toroidal flux trapped behind the ring. The resulting $\underline{J}\times\underline{B}$ forces can be balanced by the product of the ring mass and its acceleration or by a component of the radial equilibrium force if the ring is in a conical compression stage. Compression is a quasi-equilibrium state, where the radial equilibrium force nearly balances the $\underline{J}\times\underline{B}$ force of the injected toroidal flux, and allows the accelerator to match to comparatively slow power supplies, such as

moderate voltage capacitors. Without the compression stage, the accelerator can be coupled to a low capacitance, high voltage bank, however the accelerator length becomes somewhat greater. Simple flux conservation and equilibrium arguments as well as 2-D simulations show that the ring compression should be self-similar (i.e., axial extent/radial extent = a constant) so long as the plasma pressure remains low.

3) Following compression, the acceleration bank energy is stored inductively behind the compact toroid. When the compact toroid enters the straight coaxial section, shown in Fig. 3, the radial equilibrium force is supported by image currents in the wall and the $\underline{J}\times\underline{B}$ force causes an unimpeded axial acceleration. The ring is allowed to accelerate axially until the increased inductance of the ring-accelerator circuit is comparable to the inductance of the conical compression state, at which point most of the energy is in ring kinetic energy.

4) Following acceleration, the compact toroid can be focused to a small size as required for inertial fusion by insertion into a conducting funnel (see Fig. 3). The ring magnetic energy increases approximately as 1/R during focusing, at the expense of some of the kinetic energy (typically, $U_K/U_M \gg 1$). The smallest possible ring size following focusing is given approximately by $R_{final}/R_{initial} = U_{M\ initial}/U_{K\ initial}$, at which point all of the kinetic energy has been converted into ring magnetic energy.

A 2-D nonlinear resistive MHD code was used to simulate stages 1 to 3 above for a compact toroid matched to a 9.4 MJ, 120 kV capacitor bank.

The predicted characteristics of the CT accelerator are obtained using a 0-D code (RAC) which calculates the ring position and plasma properties for a lumped circuit L,C driver and conical or cylindrical coaxial electrodes. The force equation,

$$\frac{Md^2\rho}{dt^2} = L_g^1 \frac{I^2}{2} - \frac{U_m \sin\alpha}{R} - F_{drag} - F_s \qquad (1)$$

and coupled driver equation,

$$\frac{d}{dt}\left((L_x + L_a)I\right) = V_0 - \int \frac{I}{C}\,dt \qquad (2)$$

are solved assuming constant ring mass M. In eq. (1) F_{drag} is the drag force on the ring caused by penetration of the ring fields into the electrodes. The usual skin depth or velocity-dependent skin depth are used including nonlinear diffusion corrections at high B. In eq. (1), F_s is a damping force which approximates the effect of "sloshing" of the plasma to the front and rear of the ring as it is subjected to varying accelerations. In eq. (2) L_x is the external inductance and $L_a = \int L_g^1 \rho\,dt$ is the inductance of the accelerator.

The RAC code also solves the volume average magnetic and plasma energy equations,

$$\dot{U}_m = P_{\substack{magnetic\\compression}} - P_{ohmic} \qquad (3)$$

$$\dot{U}_p = P_{\substack{plasma\\compression}} + P_{ohmic} + P_s - P_{radiation} - P_{conduction} \qquad (4)$$

where U_p includes both the thermal energy of the plasma and the potential energy of each ion charge state. Plasmas composed of H and O and H and Xe ions are considered. Rate equations are solved to determine the charge-state populations of the O and Xe ions using analytical approximations for the rate coefficients. The ohmic heating term P_{ohmic} is calculated using U_m, the ring dimensions and the plasma temperature and effective charge state.

In eq. (4), P_s describes irreversible heating of the plasma due to "sloshing", $P_{radiation}$ is the radiation power calculated for each ion species assuming a two level ion and using analytical approximations for the resonance excitation rate coefficients. Reabsorption of line radiation is approximately accounted for using the larger volume averaged escape probability based on Doppler or Voight profiles. The conduction power $P_{conduction}$ in eq. (4) is calculated from the cross field, ion thermal conductivity for $\beta < 0.2$. As β approaches $\beta_{max} = 0.2$, the maximum stable β, the plasma conductivity is allowed to increase to the electron conductivity along B with an effective conduction length equal to the CT minor circumference. The increased conductivity is assumed to arise from pressure driven interchange modes which "scramble" the magnetic surfaces for $\beta > \beta_{max}$.

Calculations of possible accelerator parameters using the RAC code are subjected to the constraint that the acceleration factor $\kappa = M\rho/(U_m/L)$ must be kept less than β_{max} to avoid strong excitation of the Rayleigh-Taylor instability. A usually less restrictive constraint must also be satisfied $\kappa_{slip} < 1$ where $\kappa_{slip} = B^2_{acc}/B^2_{CT}$ to avoid "blow by" of the accelerating field.

A possible accelerator configuration calculated using the RAC code and which satisfies the above κ constraints is summarized in Table 1. The simulations show formation, compression and acceleration, as described previously.

TABLE 1. Phased acceleration and focusing of Shiva-Star driver (9.36 MJ, 120 kV, 1296 μF)*

Parameter	Unit	Initial Conditions	After Phase 1: Compression	After Phase 2: Acceleration
C	μF	1.3 (3)		
L_x	nH	40		
V_0	kV	120		
Δ	cm	15	1.7	1.7
α	rad	π/2		
ρ_0	cm	50		
R	cm	50	5.7	5.7
M	g	1 (-4)		
U_M	MJ	0.04	0.19	0.19
B	MG	0.013	0.77	0.77
t	μs	0	10.0	10.5
I	MA	0	14.0	3.5
L	nH	40	67	270
U_{cap}	MJ	9.4	1.9	1.6
U_L	MJ	0	6.9	1.7
U_K	MJ	0	0	5.0
V_r	cm/μs	0	0	1000.0
E_k	eV/amu	0	0	1.9 (6)
ℓ_{acc}	cm			341.0

The high force per unit mass combined with the large number of particles in the compact toroid allow for very compact accelerators capable of output energies in the multi-megajoule range. For example, results of 0-D code calculations for the 9.4 MJ bank are shown in Table 1. Note that 5 MJ of the available 9.4 MJ are converted into ring kinetic energy in an accelerator less than 4 m in length. The time dependence of ring parameters during the final focus stage is shown in Fig. 4. If a target were placed in the path of the ring at the point where the ring radius reaches 0.75 cm, the incident power density would be 5 x 10^{15} W/cm^2, which is approximately the conditions needed for inertial fusion.

The delivery of a high power density to the target area does not guarantee a workable system. The energy must be properly coupled to the target to allow an efficient, symmetric and stable implosion. The CTs described above can meet this criteria, provided they have been accelerated to velocities exceeding 10^9 cm/s and focused to approximately 1 to 2 cm diameter. One further condition must be met to ensure efficient coupling to the target; the kinetic energy of the CT must greatly exceed the magnetic energy. If $U_K/U_M >> 1$, then the plasma of the toroid can be treated as a space charge neutralized ion beam, having a range in the target material dictated by the ion specie and velocity. Threshold velocities of 10^9 cm/sec are required, and 3 x 10^9 are preferred. At 3 x 10^9 cm/s, the ring ions carry 5 MeV/nucleon, yielding 1.1 GeV if one is accelerating uranium, and 20 MeV for helium ions.

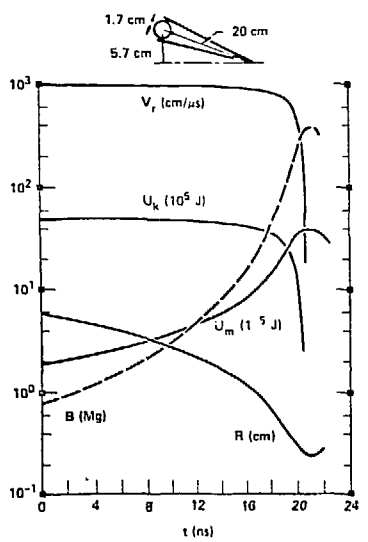

Figure 4

The above discussion assumes that the effects of the magnetic field on the deposition of ring ions in the target are negligible. This assumption is probably correct only in the limit $U_K/U_M >> 1$. When $U_K \sim U_M$, the magnetic field provides substantial rigidity to the ring during a collision with a solid body (the structural integrity of the ring is what permitted acceleration of the ring as a coherent object). Even when the ion gyroradius $\rho_i = V_{CT}/\Omega_{ci}$ ($\Omega_{ci} = eB/m_{ic}$ = ion

gyrofrequency in the CT magnetic field, V_{CT} = CT velocity) is large compared to the ring radius, the electrons tend to remain tied to the field lines and cause large space charge induced electric fields that retard ion motion across the magnetic field. Thus, the coupling to the target will be quite different, and most likely not as efficient. Therefore, the constraint of keeping $U_K/U_M >> 1$ is a key point in this scheme.

If the CT meets the acceleration and focusing constraints, target design is identical to light ion and heavy ion ICF designs. The flexibility in ion choice has already been discussed; the actual selection now depends on ion range considerations. Figure 5 indicates the range for both uranium and helium accelerated to 3 x 10^9 cm/s, and one notes a factor of three increase in range for helium. This translates into a lower energy density delivered to the target, and therefore less implosion drive. Therefore, for a fixed ion velocity, the heavier ions are preferred for target considerations.

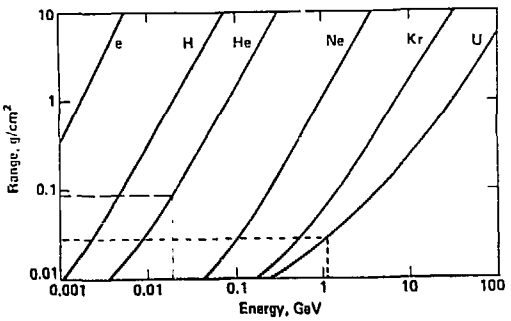

Figure 5

Both the Light and Heavy Ion Beam ICF Programs have proposed target coupling schemes using direct and indirect drive. The direct drive approach uses the ion beam to directly heat the ablator of the target, driving it inward to compress and ignite the DT fuel. An obvious difficulty with this approach is the required uniformity of beam illumination on the target surface, a requirement that must be met to insure that the implosion is symmetric and spherical. A nonuniform beam also poses the potential of heating and ablating more material from one part of the surface than another, perhaps giving rise to hydrodynamic instabilities and mixing of contaminants into the fuel. Indirect drive can reduce the deleterious effects of a nonuniform beam. The preferred approach for indirect drive is to deposit the ions in a hohlraum, converting them to thermal x-rays.

Curves predicting gain (fusion yield over source input) as a function of input energy, spot size and ion range have been published for both single and double shell targets.[7] The curves are a compendium of many 1- and 2-D computer calculations, with factors included to cover asymmetries, conversion factors and couping efficiencies. As new physics models are introduced to the codes and/or experimental data is obtained from the lasers, the information in these plots is updated. Thus the curves should be treated as guidelines, although they represent the best estimate to date. The family of curves plotted for ion beams, Fig. 6a and 6b, are a function of $r^{3/4}R$, where r is the radius of the beam at the target and R is the ion range. Examples for helium and uranium are marked on the curves, indicating a moderate gain of 60 for 5 MJ of uranium, but 10 MJ of helium is required to attain the same gain, due to its longer range.

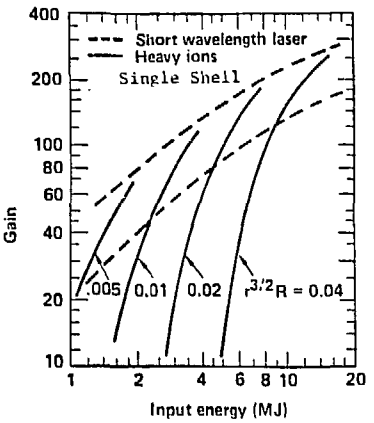

Figure 6a

The efficiency of the driver must be considered when one is evaluating the economic potential of a source. An indication of required efficiency (or target gain needed) can be obtained from the following simple relation,

$$G*\eta = 10$$

where G = target gain and η = efficiency of the source. The gain curves have suggested a gain of 60 for a 5 MJ ion beam delivered to the target and the efficiency of generating, accelerating and delivering a CT is ~50%. This yields a $G*\eta$ product of 30, easily satisfying the above criteria. One might be tempted to reduce the required target gain and therefore the delivered energy of the CT, but unforeseen practical constraints may do that in any event, and so the factor of three

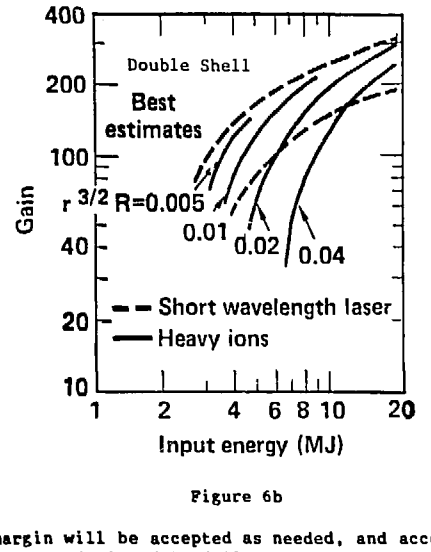

Figure 6b

margin will be accepted as needed, and accelerators designed to deliver 5 MJ.

Propagation of the CT to the Target

A number of possibilities exist for propagating the CT (or multiple CT's) across the reactor vessel and to the target. If the reactor vessel is evacuated, CT's can propagate a distance determined by the ratio of the ring expansion velocity, $\sim V_{Alfven} = B_{CT}/\sqrt{4\pi\rho_{CT}}$, to the ring directed velocity V_{CT} (see Fig. 7a). This option requires large ratios of kinetic to magnetic energy:

$$\frac{U_K}{U_M} > \left(\frac{\ell}{R}\right)^2 \sim 4 \times 10^4$$

where ℓ = range ~ 200 cm, R = ring radius ~ 1 cm.

If the reactor vessel is filled with a low density gas, the resulting shock wave and over-pressure caused by the ring's passage through the gas can provide a force that prevents expansion of the rings (see Fig. 7b), or can cause radial focusing of the rings in an increasing density gradient (this is referred to as dynamic focusing). An estimate of the required kinetic to magnetic energy ratio for dynamic focusing over a range ℓ is

$$\frac{U_K}{U_M} \gtrsim 10 \sqrt{\frac{\ell}{r}} \sim 150 \text{ for } P = 200 \text{ cm}$$

$$R = 1 \text{ cm}$$

to avoid excessive energy losses in transit. This ratio of kinetic to magnetic energy is a more realistic possibility than that required by inertia-limited focusing in a vacuum, although there are more uncertainties related to the ring interaction with the gas (e.g., excessive ring heating in the presence of the high temperature plasma behind the shock front).

The least restrictive option in terms of ring parameters is to simply extend a disposable cylindrical or conical outer electrode from the wall of the reactor vessel to the target (see Fig. 7c). This could be accomplished by forming a hollow liquid lithium jet, or possibly extending a solid lithium pipe. To simplify the task of striking the target, at least for schemes requiring only one incident CT, the pellet could be introduced at the tip of the jet before injection.

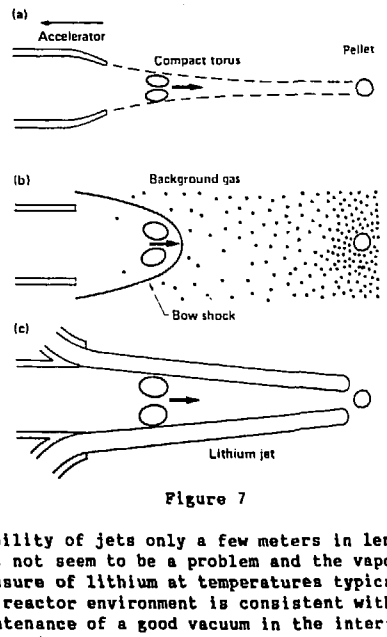

Figure 7

Stability of jets only a few meters in length does not seem to be a problem and the vapor pressure of lithium at temperatures typical of the reactor environment is consistent with maintenance of a good vacuum in the interior of the jet. The advantages of the disposable electrode method are that it places no strong constraints on the reactor vessel environment (moderately high gas pressures could be tolerated) nor on the kinetic to magnetic energy ratio of the rings.

Pulse Rate of the Accelerator

The repetition rate for the accelerator is limited by the rate at which energy can flow into the accelerator power supply (e.g., a moderate voltage capacitor bank such as SHIVA*) and by the rate at which waste heat can be removed from the accelerator structure. For example, a 10 MJ accelerator bank pulsed 3 times per second would require a steady input

of 30 MW of electrical power to the charging power supplies which should be easily achievable. The waste heat may be more of a problem because of the relatively small dimensions of the accelerator, especially in the coaxial run-down section where the inductively stored energy from the compression stage is converted to ring kinetic energy. Typical dimensions of the coaxial section would be radius R = 5 cm, length ℓ = 5 meters for a total surface area of about 3 m^2. Assuming 50% efficiency and that all of the waste energy was absorbed in the coaxial section, the average loading for the example alone is 5 MW/m^2. If the thermal stresses are excessive, the small accelerator dimensions and presumably low cost would allow use of more than one accelerator to lower the average wall loading.

Reactor Configuration

Assuming that the disposable electrode technique is used to propagate the CT's to the center of the reactor vessel, the constraints imposed by propagation on vessel diameter and gas pressure are minimal. A number of reactor configurations could then be employed. For instance consider the lithium fall concept developed at LLNL which was a flowing curtain of liquid lithium to absorb the fluence of high energy neutrons and blast effects from the fusion explosion. Possible parameters for such a reactor are shown in Table 2.

TABLE 2.

Accelerator Parameters	
Input energy	10 MJ
CT kinetic energy	5 MJ (50% efficiency)
CT mass	10^5 g
CT velocity	3×10^9 cm/sec
Accelerator length	5 meters
Pulse rate	3 cycles/sec
Ion species	U^+
Reactor Parameters	
Gain	60
Yield	300 MJ/explosion
Average fusion power	900 MJ/sec
Net electric power output	270 MW
Inner radius at Li fall	75 cm
Outer radius of Li fall	175 cm
Reactor vessel radius	3 meters
Reactor vessel height	5 meters
Power density	6.4 MW/m^3

CONCLUSION

If the CT accelerator is successful in reaching the energy and power density requirements for inertial fusion, then it appears possible to use such an accelerator as a compact, inexpensive driver for an ICF reactor. Further, the size of the reactor can be reduced from those presently proposed for ICF by virtue of the CT accelerator's cost and efficiency. A number of possibilities exist both for propagating the accelerated CT to the target and for depositing the ring energy in the target in a useful form. The technological constraints placed on the accelerator by the rapid repetition rate should not pose any fundamental difficulties. The predicted high efficiency for the accelerator (~ 50%) should allow the use of comparatively simple, moderate gain pellets of fairly low yield, and provide an economical system of electrical production in the few hundred MW regime.

ACKNOWLEDGEMENTS

Work performed under the auspices of the U.S. D.O.E. by Lawrence Livermore National Laboratory under contract #W-7405-Eng-48.

REFERENCES

1. W. C. Turner, G. C. Goldenbaum, E. H. A. Granneman, J. H. Hammer, C. W. Hartman, D. S. Prono, J. Taska, Phys Fluids 26 (7), 1965 (July 1983).
2. M. Yamada, et al., Phys. Rev. Lett. 46, 188 (1981).
3. G. C. Goldenbaum, H. J. Irby, Y. P. Chong, G. W. Hart, Phys. Rev. Lett. 44, 393 (1980).
4. T. R. Jarboe, et al., Phys. Rev. Lett. 45, 1264 (1980).
5. K. Watanabe, et al., J. Phys. Soc. Japan 50, 1823 (1981).
6. C. W. Barnes, et al., Nuclear Fusion 24 (3), 267 (1984).
7. R. O. Bangerter, J. W. K. Mark, D. J. Meeker, D. L. Judd, "The Influence of Target Requirements on the Production, Acceleration, Transport and Focusing of Ion Beams", in Proceedings of the 4th Intl. Top. Conf. on High Power Electron and Ion-Beam Research and Tech., June 24-July 3, 1981, Palaiseau, France.